

REPORT DOCUMENTATION

AD-A255 345

oved
704 0185

2

1. AGENCY USE ONLY (Leave blank)		2. REPORT DATE	3. REPORT TYPE AND DATES COVERED Reprint	
4. TITLE AND SUBTITLE Title show. on Reprint			5. FUNDING NUMBERS DAA03-89-K-0026	
6. AUTHOR(S) Authors listed on Reprint				
7. PERFORMING ORGANIZATION NAME(S) AND ADDRESS(ES) Univ. of Maryland College Park, Maryland 20742			8. PERFORMING ORGANIZATION REPORT NUMBER	
9. SPONSORING MONITORING AGENCY NAME(S) AND ADDRESS(ES) U. S. Army Research Office P. O. Box 12211 Research Triangle Park, NC 27709-2211			10. SPONSORING / MONITORING AGENCY REPORT NUMBER ARO 26278-36-EL	
11. SUPPLEMENTARY NOTES The view, opinions and/or findings contained in this report are those of the author(s) and should not be construed as an official Department of the Army position, policy, or decision, unless so designated by other documentation.				
12a. DISTRIBUTION AVAILABILITY STATEMENT Approved for public release; distribution unlimited.			12b. DISTRIBUTION CODE	
13. ABSTRACT (Maximum 200 words) ABSTRACT SHOWN ON REPRINT 92 9 02 104 DTIC ELECTE SEP 4 1992 92-24440 464-1 8pl				
14. SUBJECT TERMS			15. NUMBER OF PAGES	
			16. PRICE CODE	
17. SECURITY CLASSIFICATION OF REPORT UNCLASSIFIED	18. SECURITY CLASSIFICATION OF THIS PAGE UNCLASSIFIED	19. SECURITY CLASSIFICATION OF ABSTRACT UNCLASSIFIED	20. LIMITATION OF ABSTRACT UL	

Confined phonon modes and hot-electron energy relaxation in semiconductor microstructures

S Das Sarma†, V B Campos†‡, M A Stroscio† and K W Kim§

†Joint Program for Advanced Electronic Materials, Department of Physics,
University of Maryland, College Park, MD 20742 USA

‡US Army Research Office, PO Box 12211, Research Triangle Park, NC 27709,
USA

§Department of Electrical and Computer Engineering, North Carolina State
University, Raleigh, NC 27695, USA

Abstract. The role of confined phonon modes in determining the energy relaxation of hot electrons in low-dimensional semiconductor microstructures is discussed within a dielectric continuum model for the LO phonon confinement and a long wavelength Fröhlich model for the electron-phonon interaction. Numerical results are provided for the hot-electron relaxation rate as a function of electron temperature and density for GaAs quantum wells and quantum wires by taking into account emission of slab phonon modes. Comparison with existing experimental results shows some evidence for slab phonon emission in *inter-subband* electronic relaxation in reasonably narrow quantum wells. It is argued that most experiments can be interpreted in terms of an electron-bulk phonon interaction model (i.e. by taking into account the effect of confinement only on the electrons and assuming the phonons to be the usual bulk three-dimensional phonons) because a number of important physical processes, such as screening, the hot phonon effect, phonon self-energy correction etc. make it difficult to distinguish quantitatively between various models for phonon confinement, except perhaps in the narrowest (< 50 Å) wells and wires. Detailed numerical results for the calculated *intra-subband* relaxation rate in GaAs quantum wires are provided within the slab phonon and the electron temperature model, including the effects of dynamical screening, quantum degeneracy and non-equilibrium hot phonons.

1. Introduction

A large number of theoretical papers have recently appeared [1-21] on the subject of interaction between free electrons and optical phonons in *confined* low-dimensional semiconductor structures such as semiconductor heterostructures, quantum wells, superlattices and quantum wires. While it is well established [1] that the effect of quantum confinement on the electronic degrees of freedom must be included in any reasonable theoretical model of electron-phonon interactions in these microstructures, the recent emphasis in the literature has been on the inclusion of confinement effects on the phonon modes of the structures and the consequent modification of the Fröhlich Hamiltonian describing the electron-phonon interaction in the system. Because Fröhlich interaction plays an important quantitative role in determining many aspects of the electronic properties (e.g. electron mobility, hot-electron relaxation, inelastic mean free path, polaron effective mass) of microstructures, the possible influence of confined phonon

modes in semiconductor microstructures is of some interest. The purpose of this paper is to discuss the quantitative role of confined phonon modes from the perspective of one particular class of phenomena, namely, the hot-electron energy relaxation process in quantum wells and wires. Our main concern in this article is the role of confined phonon modes in the energy relaxation of hot electrons in GaAs microstructures with the particular emphasis on qualitative and quantitative understanding of recent experimental results [22-30].

The most unambiguous evidence for the existence of confined phonon modes in microstructures comes from Raman scattering experiments [22-24] in thin GaAs-AlAs superlattices where confinement effects on both the acoustic phonons [22] and optical phonons [23, 24] have directly been observed for layer thicknesses typically below 50 Å. Unfortunately, such Raman measurements cannot tell us much about the role of confined phonon modes in determining various electronic properties. In addition, the Raman measurements (and this limitation applies also to all of the 'so-called' first principles or microscopic lattice-dynamical calculations) are necessarily on superlattices whereas the electronic experiments

†On leave from Departamento de Física, Universidade Federal de São Carlos, SP, Brazil.

are most commonly done on single heterostructures or quantum wells (or on fairly thick superlattices). More important than the issue of the existence of confined phonon modes is the question of their quantitative role in the electron-phonon interaction Hamiltonian. There are two related theoretical questions:

(i) How much of an error is one making by assuming that the confined electrons interact only with the regular three-dimensional bulk phonons of the relevant semiconductor?

(ii) If the confinement effect on phonons is indeed important (i.e. the bulk phonon model is a bad one in a particular experimental situation), what is the correct model for calculating the electron-phonon interaction Hamiltonian in semiconductor microstructures?

In the following, we address, to a limited extent, both these issues in the specific context of the hot-electron energy relaxation problem.

There have been two proposed macroscopic theoretical models for studying confined phonon modes in semiconductor microstructures. While both treat the confined phonon modes as standing waves in the microstructure, the two models differ significantly in their macroscopic boundary conditions. One of them (to be referred to as the electrostatic or the slab mode model) uses the usual electromagnetic boundary conditions at interfaces demanding the continuity of the tangential component of the E -field (we take z to be the direction perpendicular to the well interface and q to be the two-dimensional wavevector in the xy plane) and the normal component of the D -field. In the other model (to be referred to as the mechanical or the guided mode model), one uses a hydrodynamic description for the lattice-vibration amplitude and applies the mechanical boundary conditions. Details of the models have been extensively discussed and debated in the literature [9, 13-18]. For our purpose it is sufficient to state that the electrostatic model has the electric potential, $\phi(q, z)$, associated with the lattice polarization field vanishing at interfaces, whereas in the mechanical model it is the electric field component $E_z(q, z)$ (or, equivalently the z component of the optical vibration amplitude) which vanishes at the interfaces. Since $E_z = -\partial\phi/\partial z$, the two models indeed have very different implications for the Fröhlich electron-phonon interaction, which is basically given by $-e\phi(z)$. The electron-phonon interaction matrix element in a quantum well of width a , with $0 \leq z \leq a$, is given within the electrostatic approximation by

$$M_{ij}^{(m)}(q) = [(4\pi e^2/Q_m^2)\omega_{LO}/2\kappa(1/\epsilon_\infty - 1/\epsilon_0)\kappa(2/a)\beta_{ij}^{(m)}]^{1/2} \quad (1)$$

where

$$Q_m^2 = q^2 + q_m^2 \quad q_m = m\pi/a \quad (2)$$

and

$$\beta_{ij}^{(m)} = \int_0^a dz \zeta_i^*(z) \sin(q_m z) \zeta_j(z). \quad (3)$$

Note that the condition $\phi(z) = 0$ at $z = 0, a$ produces discrete phonon wavevectors $q_m \equiv q_m = m\pi/a$ in the z direction with $m = 1, 2, 3$, etc. This follows from demanding that $\phi(z) \sim \sin(q_z z) = 0$ at $z = a$. In equations (1)-(3), Q is the three-dimensional phonon wavevector; i, j are electronic subbands described by wavefunctions $\zeta_i(z)$ and $\beta_{ij}^{(m)}$ is the electron-phonon interaction form factor which takes into account both electron and phonon confinement.

For the mechanical model, (3) is modified to

$$\beta_{ij}^{(m)} = \int_0^a dz \zeta_i^*(z) \cos(q_m z) \zeta_j(z) \quad (4)$$

with $q_m = m\pi/a$ (and $m = 1, 2, 3, \dots$ etc) because the boundary condition leading to discrete values of q_z are now applied on the electric field, rather than on the potential itself. Note that the ionic optical displacement and the potential are given by $u_z \sim \cos(q_z z)$ and $\phi \sim \sin(q_z z)$ in the slab model, whereas these are reversed in the guided mode model. Another way of stating the difference between the two models is to point out that in the guided mode model $u_z = 0$ at the interface, whereas in the slab model it is the tangential or the in-plane component of optical-vibration amplitude which is zero at the interface.

Much has been written on the relative merits of these two rather simple macroscopic models. Without repeating various published arguments in detail, we just make some brief remarks here:

(i) In general, the electron-phonon interaction strength decreases with an increase in the confined phonon mode number, m , because of the increase in the number of nodes of the confinement function. Calculations show that it often suffices to have only the lowest discrete mode allowed under the symmetry of the situation. We adopt this approximation in all our calculations.

(ii) If the quantum well (or the wire) is symmetric so that the electronic wavefunctions $\zeta_i(z)$ are parity eigenstates, then $\beta_{ij}^{(m)} = 0$ whenever $i + j + m = \text{even}$ (odd) for the slab (guided) modes, where we classify the quantum well wavefunction by their parity with i, j even or odd indicating the corresponding symmetry states. Note that this has non-trivial consequences for intra-subband scattering ($i = j$) for which the lowest slab mode ($m = 1$) can participate but the lowest guided mode cannot. Thus, purely on the grounds of symmetry (assuming, of course, that real quantum well systems are symmetric so that parity is a good quantum number) we conclude that the intra-subband scattering rate due to slab modes is substantially stronger than that due to the guided modes. For inter-subband ($i = j \pm 1$) relaxation, on the other hand, the guided modes produce much stronger scattering than the slab modes because the lowest ($m = 1$) guided mode can participate in the inter-subband relaxation whereas the lowest slab mode cannot. This also indicates that, other things being equal, for the slab model, intra-subband relaxation via LO phonon emission should be substantially faster than the inter-subband relaxation, and vice versa for the guided model. Thus, a

comparison between intra- and inter-subband energy relaxation of hot carriers in quantum wells should enable one to distinguish between the two alternative models for phonon confinement in semiconductor microstructures. This criterion clearly favours the electrostatic or the slab model because, experimentally [25–28], intra-subband relaxation in GaAs quantum wells is approximately an order of magnitude faster than the inter-subband relaxation process. (The situation is not as simple as it appears because interface phonons which decay exponentially away from the interfaces also contribute to the scattering, complicating somewhat, but not substantially, these simple symmetry considerations based only on the slab and guided modes.)

(iii) In addition to the slab (or guided) modes which exist in the *bulk* of the quantum well (i.e. $\phi \sim \sin(qz)$; $u_z \sim \cos(q_z z)$), one could also have in the electrostatic model surface or interface phonon [31] modes whose amplitudes (and the consequent electric potential) decay exponentially away from the interfaces. Within the electrostatic model these modes arise naturally as a consequence of the boundary conditions (similar to the surface or interface plasmon problem) and are of quantitative significance for very thin ($< 30 \text{ \AA}$) wells. In the mechanical model, the guided modes have zero amplitudes at the interfaces and, therefore, strictly speaking, interface phonon modes are not allowed. This again, in our opinion, is an argument against the mechanical boundary conditions. Using the electrostatic boundary conditions, it is easy to incorporate the effect of interface phonons on the electron-phonon interaction Hamiltonian within the dielectric continuum model. As stated before, interaction between electrons and interface phonons is negligibly small except for very thin systems.

(iv) In addition to the two macroscopic models discussed above, one can, of course, calculate the electron-phonon interaction in confined structures microscopically [9, 13, 14] by using suitable lattice-dynamical models. Such calculations, while being conceptually straightforward, are computationally intensive and can be carried out only for very thin systems and, for obvious technical reasons, only in superlattice configurations. Microscopic calculations demonstrate rather convincingly [9, 15, 17] that the electrostatic slab model works very well in microstructures except for the narrowest confinement ($< 30 \text{ \AA}$) where the dielectric continuum approximation breaks down and an atomistic description becomes necessary (Motivated by the microscopic models, a new macroscopic model has been introduced recently [9] to study electron-phonon interaction in microstructures. This model is intermediate between the slab model and the guided model and combines both sets of boundary conditions in a dielectric continuum description.) In general, the microscopic calculations do not support the macroscopic mechanical guided mode model. We do mention, however, that such first-principles microscopic calculations are not practical for *directly* calculating experimentally interesting electronic properties such as energy relaxation or power loss by hot electrons, though the microscopic models have been

reasonably successful [30] in describing the experimental phonon dispersion in thin superlattices.

(v) Finally, we note that the most extensively used model [1, 11, 12] for calculating electron-phonon interaction in semiconductor microstructures has been the three-dimensional phonon approximation (3DPA) where the phonons are taken to be the usual bulk phonons of the relevant semiconductor material interacting with the low-dimensionally confined electrons. In quantum wells or heterojunctions, where the electron dynamics in the z direction is quantized, one sums over the free phonon wavevector q_z to obtain an effective two-dimensional electron-phonon interaction given by

$$M_{ij}(q, q_z) = [2\pi\omega_{LO}e^2(1/\epsilon_r - 1/\epsilon_0)]^{1/2}(q^2 + q_z^2)^{-1/2} \times \int dz \xi_i^*(z) e^{iq_z z} \xi_j(z) \quad (5)$$

which, after the sum over the free phonon wavevector q_z , leads to the following effective electron-phonon interaction matrix element:

$$M_{ij\mu\nu}^2(q) = |M_q|^2 f_{i\mu\nu}(q) \quad (6)$$

where

$$|M_q|^2 = (\pi e^2 \omega_{LO} / q) (1/\epsilon_r - 1/\epsilon_0) \quad (7)$$

and

$$f_{i\mu\nu}(q) = \int dz \int dz' \xi_i^*(z) \xi_j(z) \xi_\mu^*(z') \xi_\nu(z') e^{-iq_z(z-z')} \quad (8)$$

The 3DPA has been very successful in describing the electron-phonon interaction properties in microstructures and often produces results [10, 12, 15, 17] not very different from that given by the confined phonon model. In fact, microscopic calculations [15, 17] show that, except in the thinnest samples, 3DPA is qualitatively and semi-quantitatively quite valid in GaAs microstructures.

For brevity, we show our formulae (1–8) only for the 2D quantum well case—the quantum wire situation is similar [19, 21] with the electron being also quantized along one other (y) direction and the phonon slab modes being standing waves (described by two discrete indices) in two directions.

2. Model

With the above background, we now introduce our model for the calculations presented in this paper. We model the electron confinement entirely by an infinite-square-well potential. All our calculations are done within a Fröhlich dielectric continuum slab phonon model using the electrostatic boundary conditions. For reasons discussed in the introduction we believe that this model works very well for GaAs microstructures, except perhaps for the narrowest confinement (less than 30 \AA) where microscopic, atomistic phonon models are needed. (Microscopic calculations support our claim.) Even though we include interface phonons in some of our

calculations (for the 2D results, for example) they are mostly neglected because their effects for the system sizes we are interested in (50 Å or larger) are usually small. In fact, our quantum wire results include *only* the slab phonons and leave out the interface phonons entirely. Since the electron wavefunction vanishes (or is very small) at the interfaces where the interface phonon amplitude peaks, neglect of interface phonons is usually a good approximation [10].

We also include dynamical screening and quantum degeneracy effects throughout our calculations, providing a quantitative estimate for their importance [32, 33]. Since we are considering a finite electron density, it is important to keep these quantum effects in the theory. We also include in our theory [11, 34] the many-body phonon renormalization effect (i.e. the self-energy correction of the phonon frequencies by the electron gas) where it is appropriate. At low densities and electron temperatures, this many-body renormalization is quite important in 2D systems as has been discussed earlier in the literature [11, 33, 34]. Finally, we include hot-phonon effect [11, 32, 33, 35] in our theory through a phenomenological kinetic equation approach assuming a given value for the hot-phonon lifetime, τ_{ph} . For GaAs heterostructures, the hot-phonon effect is a very important quantitative correction [11, 36]. Throughout this paper we assume the lattice to be at zero temperature and adopt an electron-temperature model [11] for the hot electrons. Thus, our model implicitly assumes that the electrons have equilibrated amongst themselves, acquiring a hot-electron distribution at an elevated temperature T . Our task is to calculate the power loss from this hot-electron gas to the lattice as the coupled system equilibrates.

For quantum wells we take the z direction to be the confinement direction, whereas for a quantum wire we take the additional confinement to be along the y direction (i.e. infinite square well potentials along the y and z directions with the electrons being free to move along the x direction). We neglect all effects of AIAs in the barrier region in our calculations. For both quantum wells and wires, we include only the lowest phonon slab mode ($m = 1$) in our calculation. We consider only intra-subband relaxation in the lowest electronic subband of the system.

It can be shown that the power loss per hot electron due to LO phonon emission is given (including the hot-phonon effect) by the formula [11, 32]

$$\frac{P}{N} = \hbar\omega_{LO} n_T(\omega_{LO}) \sum_Q \frac{R_Q}{1 + \tau_{ph} R_Q} \quad (9)$$

where we assume the lattice to be at zero temperature with $n_T(\omega_{LO})$ the appropriate Bose factor at the hot-electron temperature T . N is the electron number density and R_Q is the energy relaxation rate at wavevector Q given by

$$R_Q = -2A|M_Q|^2 \text{Im} \chi(Q, \omega_{LO}) \quad (10)$$

Here, M_Q is the appropriate electron-slab phonon

interaction matrix element at wavevector $Q = \sqrt{(q_x^2 + q_y^2 + q_z^2)}$, and χ is the finite-temperature dynamically screened reducible electron polarizability function defined as

$$\chi = \chi_0(1 - v\chi_0)^{-1} \quad (11)$$

where χ_0 is the finite-temperature bare bubble (the Lindhard function) in the appropriate dimension and v is the electron-electron interaction including the subband quantization effect.

Due to lack of space we do not show here the detailed forms of χ_0 and v (for both the quantum well [11] and the quantum wire [21, 37]) and of $|M_Q|^2$ for the quantum wire [19, 21]. Their evaluations are standard and can be found in the literature.

In the next section we present our results based on this electron-temperature model for power loss due to slab phonon emission in GaAs quantum wells and wires in the electron-temperature range $50 \text{ K} < T < 300 \text{ K}$. After presenting a brief review of some limited (and published) quantum well results, we concentrate mostly on the GaAs quantum wire results which are completely new.

3. Results

3.1. GaAs quantum wells

A rather extensive literature exists on the role of confined phonons in hot-electron energy relaxation in GaAs quantum wells. It is well accepted that confined modes play a quantitative role in thin wells (and superlattices), generally for thicknesses less than 50 Å. (This is also consistent with the conclusions of microscopic calculations.) In particular, Jain and Das Sarma calculated [10] the intra-subband and the inter-subband hot-electron energy relaxation rate in GaAs quantum wells including effects of slab and interface modes within the electrostatic boundary conditions. Their calculation includes the phonon renormalization effect and uses $\tau_{ph} = 7 \text{ ps}$. Their results for intra-subband relaxation for two different well widths are shown in figure 1. One can see that for the 50 Å well, particularly at lower electron temperatures, slab mode effects are significant. In general, the interface phonon contributions are not significant unless the well widths are 30 Å or smaller. Jain and Das Sarma also pointed out [10] that in thin wells inter-subband energy relaxation will be substantially reduced due to parity restrictions arising from the fact that the lowest slab mode ($m = 1$) cannot participate in the process. Consequently, they found that the inter-subband relaxation rate is approximately an order of magnitude slower due to this slab mode parity restriction. In quantum wells of finite depths, the electron-phonon interaction is further weakened, making the inter-subband relaxation time (τ) around 5–10 ps, which is in excellent agreement with the available experimental results [25–27].

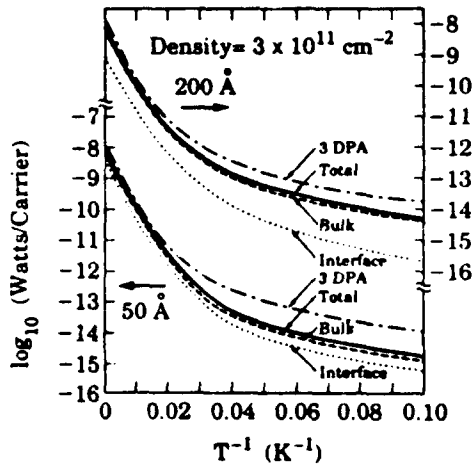


Figure 1. \log_{10} (power loss per carrier) as a function of inverse electron temperature for two quantum well widths with bulk denoting the contribution of the slab phonon modes (from [10]).

3.2. GaAs quantum wires

The main results to be presented in this paper are our new results on *intra-subband* relaxation in GaAs quantum wires due to slab phonon emission. We assume the electric quantum limit—i.e. where the lowest 1D subband is the only occupied level—and choose electron density and wire width to be consistent with this assumption. We include quantum degeneracy, finite-temperature dynamical screening, hot-phonon effect and slab modes in the calculation, but neglect phonon self-energy corrections (which are very small in 1D) and interface phonons (which are negligible except for widths 30 Å or smaller).

In figures 2(a) and (b), we show our calculated power loss per carrier for the electron density $N = 10^8 \text{ cm}^{-3}$ and for two wire widths, $L_y = L_z = 50 \text{ Å}$ and 200 Å (where L_y and L_z are the widths of the infinite-square-well confinement in the y and z directions), as a function of the inverse electron temperature. In each figure, we show results for six different theoretical approximations: classical, quantum without any screening (i.e. the χ in (10) is replaced by χ_0), quantum with static screening, and three different versions of quantum with dynamical screening—one without any hot-phonon effect (i.e. $\tau_{ph} = 0$), the other two with hot-phonon effect using two different values of the hot-phonon lifetime; $\tau_{ph} = 1$ and 7 ps ($\tau_{ph} = 7 \text{ ps}$ is the expected hot-phonon lifetime [38] in bulk GaAs). The first four approximations neglect the hot-phonon bottleneck effect and assume $\tau_{ph} = 0$. It is clear that, as in the corresponding 2D GaAs quantum well case, the hot-phonon effect is the main quantitative correction on the energy relaxation process provided $\tau_{ph} > 1 \text{ ps}$. Of course, one does not know the actual value for the hot-phonon lifetime [28] in GaAs quantum wires, but it is reasonable to expect that it is not substantially different from the bulk value of 7 ps .

In figures 2(a) and (b), we show the behaviour of our

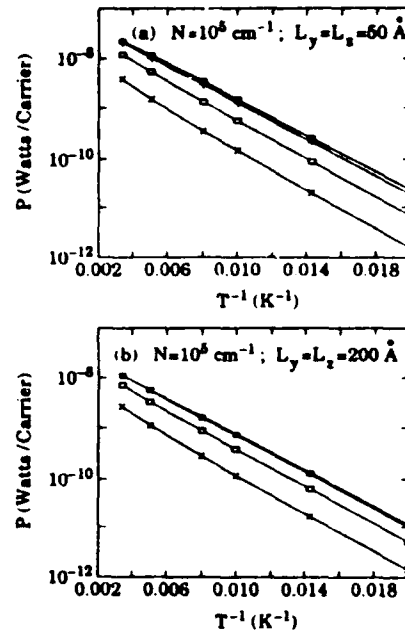


Figure 2. Power loss per carrier as a function of inverse electron temperature for a quantum wire with electron density $N = 10^8 \text{ cm}^{-3}$ and two wire widths $L_y = L_z = 50 \text{ Å}$ (a) and 200 Å (b), for six different approximations, as described in the text. (See figure 3(a) for the symbols used in the six approximations.)

calculated hot-electron energy relaxation time, τ , as a function of electron density (for a fixed wire width) and wire width (for a fixed density), respectively. To obtain τ , we note that our $\log P$ versus $1/T$ plots in figure 2 are linear in the $T = 50\text{--}300 \text{ K}$ range so that we can write (to a very good degree of approximation):

$$P = (\hbar\omega_{LO}/\tau)e^{-\hbar\omega_{LO}/k_B T} \tag{12}$$

which gives us the definition of τ , the hot-electron relaxation time. From figure 3 we see clearly that the hot-phonon lifetime is the most significant quantitative correction on the hot-electron energy relaxation in quantum wires in the regime of our interest.

Before concluding, we emphasize that our calculated τ in figure 3 is not the same as the simple electron-slab phonon scattering time [16–20] which can be calculated by using Fermi's golden rule (and which does not include quantum degeneracy, finite electron temperature and density effects, dynamical screening, hot-phonon lifetime etc). For the purpose of comparison, in figure 4 we give our calculated electron-slab phonon scattering time as a function of electron energy, E , for several different values of the quantum wire width.

4. Conclusion

In this paper we present calculated results for hot-electron energy relaxation through the emission of slab

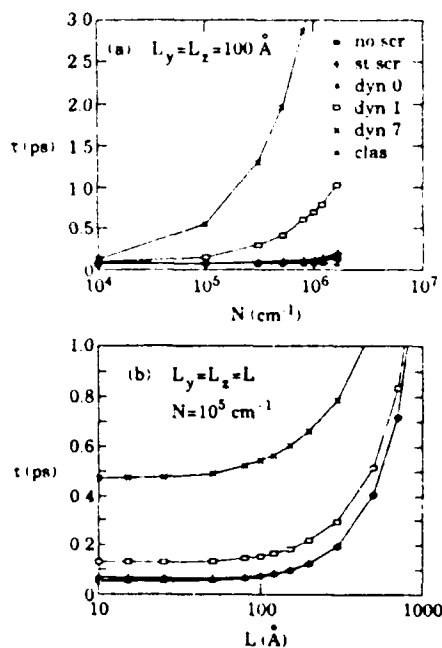


Figure 3. Calculated electronic energy relaxation time, τ , as a function of (a) electron density for a fixed quantum wire width, and (b) width for a fixed electron density for the same approximations as in figure 2. (Figure 3(a) gives the legend for the six approximations.)

phonons in GaAs quantum wires within an electron-temperature model. We also briefly review the corresponding situation for GaAs quantum wells. There are no currently available experimental results in quantum wires with which our theory can be compared. Our main conclusion is that, while quantum confinement and dynamical screening effects are both important, the most important quantitative correction for the hot-electron energy relaxation process in GaAs quantum wires arises from the hot-phonon bottleneck effect, at least for wire widths between 50 and 500 \AA and electron densities and temperatures between 10^4 and 10^6 cm^{-3} and 50 K and 300 K, respectively. We also contend that the electrostatic slab phonon model is the appropriate macroscopic

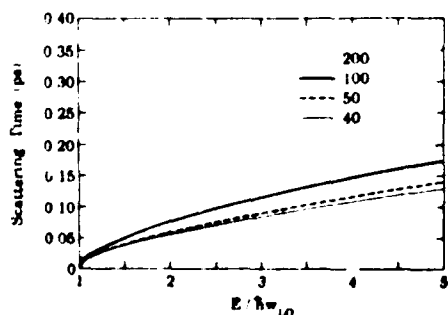


Figure 4. Calculated scattering time as a function of electron energy in quantum wires for different wire widths ($L_x = L_y = L_z$) in \AA as shown.

model for calculating hot-electron energy relaxation in confined structures. We hope that our theoretical predictions will motivate experimental work in the subject.

Acknowledgments

This work has been supported by the US-ARO and the US-ONR. VBC would like to thank the financial support from FAPESP (Fundação de Amparo à Pesquisa do Estado de São Paulo, Brazil). SDS acknowledges receipt of a Distinguished Research Fellowship of the Graduate School of the University of Maryland.

References

- [1] Mason B A and Das Sarma S 1987 *Phys. Rev. B* **35** 3890
Das Sarma S and Mason B A 1985 *Phys. Rev. B* **31** 5536, 1985 *Ann. Phys., N.Y.* **163** 78
- [2] Lassnig R 1984 *Phys. Rev. B* **30** 7132
- [3] Piddoch F A and Ridley B K 1985 *Physica B+C* **134** 342
- [4] Sawaki N and Akasaki T 1985 *Physica B+C* **134** 494
- [5] Babiker M 1986 *J. Phys. C: Solid State Phys.* **19** 683
- [6] Sawaki N 1986 *Surf. Sci.* **170** 537, 1986 *J. Phys. C: Solid State Phys.* **19** 4965
- [7] Wender L and Pechstedt R 1987 *Phys. Status Solidi b* **141** 129
Wender L 1985 *Phys. Status Solidi b* **129** 513
- [8] Trallero Giner C and Comas F 1988 *Phys. Rev. B* **37** 4583
- [9] Huang K and Zhu B 1988 *Phys. Rev. B* **38** 2183 and 13377
- [10] Jain J K and Das Sarma S 1989 *Phys. Rev. Lett.* **62** 2305
- [11] Das Sarma S, Jain J K and Jalabert R 1990 *Phys. Rev. B* **41** 3561
- [12] Jalabert R and Das Sarma S 1989 *Phys. Rev. B* **40** 9723
Jalabert R 1989 *PhD Thesis* University of Maryland, USA and references therein.
- [13] Akera H and Ando T 1989 *Phys. Rev. B* **40** 2014
- [14] Bechstedt F and Gerecke H 1989 *Phys. Status Solidi b* **154** 565, 1989 **156** 151; 1990 *J. Phys. Condens. Matter* **2** 4363
- [15] Mori K and Ando T 1989 *Phys. Rev. B* **40** 6175
- [16] Ridley B K 1989 *Phys. Rev. B* **39** 5282
- [17] Rudin S and Reinecke T L 1990 *Phys. Rev. B* **41** 7713
- [18] Ridley B K and Babiker M 1991 *Phys. Rev. B* **43** 9096
- [19] Strosio M A 1989 *Phys. Rev. B* **40** 6428
Strosio M A, Kim K W and Littlejohn M A 1991 *Proc SPIE* **1362** 562
- [20] Constantinou N C and Ridley B K 1990 *Phys. Rev. B* **41** 10622 and 10627
- [21] Campos V B, Das Sarma S and Strosio M 1991 *Phys. Rev. B* to be published
- [22] Colvard C, Merlin R, Klein M V and Gossard A C 1980 *Phys. Rev. Lett.* **43** 298
- [23] Sood A K, Menendez J, Cardona M and Ploog K 1985 *Phys. Rev. Lett.* **54** 2111 and 2115
- [24] Farol G, Tanaka M, Sakaki H and Horikoshi Y 1988 *Phys. Rev. B* **38** 6056
- [25] Selmeir A, Hübner H J, Abstreiter G, Weimann G and Schlapp W 1987 *Phys. Rev. Lett.* **59** 1345
Selmeir A, Hübner H J, Wörner M, Abstreiter G, Weimann G and Schlapp W 1988 *Solid-State Electron.* **31** 767

- [26] Tatham M C, Ryan J F and Foxon C T 1989 *Solid-State Electron.* 32 1497; 1989 *Phys. Rev. Lett.* 63 1637
- [27] Ryan J F and Tatham M 1989 *Solid-State Electron.* 32 1429
- [28] Oberli D Y, Wake D R, Klein M V, Klem J, Henderson T and Morkoc H 1987 *Phys. Rev. Lett.* 59 696
- [29] Tsen K T, Joshi R P, Ferry D K and Morkoc H 1989 *Phys. Rev. B* 39 1446
- [30] Menendez J 1989 *J. Lumin.* 44 285 and references therein
- [31] Fuchs R and Kiewer K J. 1965 *Phys. Rev.* 140 A2076
Licari J J and Evrad R 1977 *Phys. Rev. B* 15 2254
- [32] Senna J R and Das Sarma S 1987 *Solid State Commun.* 64 1397
- [33] Das Sarma S, Jain J K and Jalabert R 1987 *Phys. Rev. B* 37 1228; 1988 *Phys. Rev. B* 37 4560 and 6290; 1988 *Solid-State Electron.* 31 695
- [34] Jain J K, Jalabert R and Das Sarma S 1988 *Phys. Rev. Lett.* 60 353
- [35] Price P J 1985 *Physica B+C* 134 164
Kocevar P 1985 *Physica B+C* 134 155
- [36] Shah J, Pinczuk A, Gossard A C and Weigmann W 1985 *Phys. Rev. Lett.* 54 2065
- [37] Li Q P and Das Sarma S 1991 *Phys. Rev. B* 43 11768; 1990 *Phys. Rev. B* 41 10268; 1989 *Phys. Rev. B* 40 5860
- [38] Kash J A, Tsang J C and Hvam J M 1985 *Phys. Rev. Lett.* 54 2151

Accession For	
NTIS GRA&I	<input checked="" type="checkbox"/>
DTIC TAB	<input type="checkbox"/>
Unannounced	<input type="checkbox"/>
Justification	
By _____	
Distribution/	
Availability Codes	
Dist	Avail and/or Special
A1	20

DTIC QUALITY INSPECTED 1